Instability of a strong pulse current in a tungsten plate

1997 J. Phys.: Condens. Matter 9 2065

(http://iopscience.iop.org/0953-8984/9/9/018)

J. Phys.: Condens. Matter **9** (1997) 2065–2074. Printed in the UK PII: S0953-8984(97)76581-0

Instability of a strong pulse current in a tungsten plate

A B Rinkevich and V V Ustinov

Institute for Metal Physics, Ural Division of Russian Academy of Sciences, 18 S Kovalevskaya Str, GSP-170 Ekaterinburg, 620219 Russia

Received 23 July 1996, in final form 11 November 1996

Abstract. The instability of a strong pulse current is observed in a plate of pure tungsten. The instability appears at low temperatures if the plate is placed in a high magnetic field parallel to the current direction. The magnetic field of the alternating current in the sample is detected by making use of a Hall probe. The inherent frequencies of the instability currents are some tens of hertz. Their amplitude ranges up to about hundreds of milliamperes. The primary directions of the instability fields are along the steady magnetic fields, so that the instability currents have a component at right angles to the initial current direction. There is a threshold value of the amplitude of the pulse current at the beginning of instability. It has been found that the threshold value depends on the steady magnetic induction and is reduced significantly when the induction increases.

The amplitude of the instability currents under study exhibits features of the dynamical chaos regime. The conversion into the chaos regime is effected by the formation of turbulent time intervals intermittent with laminar time intervals. It was found experimentally that the occurrence of the current instability is accompanied by ultrasonic oscillations.

The observed instability is attributable to the fact that the magnetic field of the current pulses changes the trajectories of electrons. A set of equations has been proposed in order to explain the oscillatory behaviour of the fields of instability. This set contains two differential equations of parabolic type like the distributed parameter system with diffusion.

1. Introduction

Some types of electric current instability are known to exist in metals and semimetals. If the material of a conductor possesses a strong magnetoresistance, the action of the inhomogeneous intrinsic magnetic field of the current leads to redistribution of the current density across the section of that conductor [1, 2]. Excitations of galvanomagnetic [3] or elastic [4] waves exist. Excitation of auto-oscillations has been predicted in thin wires with open Fermi surfaces [5]. Oscillations in the voltage drop were observed in the fixed-current regime for the sample of compensated metal under static skin-effect conditions [6].

The existence of a group of electrons, whose trajectories are localized not far from the line where the inhomogeneous magnetic field changes its sign, leads to an instability of a peculiar type. This group causes a magnetodynamic non-linearity to appear in the current redistribution in a metal and therefore results in distortion of the voltage–current characteristics [7]. The magnetodynamic type of instability is observed in a thin tungsten plates [8]. As suggested in [9], a structure consisting of current layers is shown to exist in a compensated metal under similar conditions. This structure has opposite current directions in the neighbouring layers. The trapped electrons cause a square-law rise in the voltage drop versus current. The oscillational deviations are superimposed on the voltage–current characteristic with a decrease in the number of electrons with Larmor orbits. The instability

0953-8984/97/092065+10$19.50

of the current layers results in auto-oscillations in the voltage drop in the fixed-current regime. If a high external magnetic field is imposed parallel to the direct current in a plate, then a group of electrons trapped by the resulting inhomogeneous magnetic field appears [10]. Under these conditions, stratification of current should occur and oscillations arise when redistribution of the current density takes place.

As shown in [11], the magnetic field suppresses the instability if the external field and the magnetic field due to the current are of the same order; this displaces the threshold values to stronger currents. The instabilities of a pulsed current in metals and the influence of the magnetic fields on these instabilities have yet to be investigated. This is the goal of the present paper. The use of a pulsed current makes it possible to generate instabilities whose frequency spectrum corresponds to the spectrum of the current pulses. Also, the employment of the short pulses enables us to decrease the sample heating essentially.

2. Experimental technique

The tungsten single-crystal plate was placed in a helium cryostat at the temperature $T = 4.2$ K. The magnetic field direction of the superconducting solenoid was in the plate plane along the [001] crystal axis. Lengthwise the pulse current was passed along the same z axis. The Hall probe was placed on the sample plane in such a way that it is capable of measuring the z component of the magnetic field. In this position, no signal arises on the potential contacts of the Hall probe because of the field due to the current pulses, if this current flows along the z axis. In operation the external magnetic induction B_0 can be changed up to 8 T. Furthermore, the parameters of the current pulse were varied: its amplitude J_M up to 80 A, its duration τ_J from 30 to 160 μs, and its repetition frequency F from 20 to 200 Hz. The leading edge of the current pulse was 8 μs, and the trailing edge was 12 μs. The voltage from the Hall probe, connected with the current instability, was measured as described below.

The tungsten sample has a plate shape of dimensions 24 mm $\times$ 6 mm $\times$ 0.5 mm; its faces are parallel to the (100) crystal planes. The residual resistance ratio of the crystal is about 10^5. The plate was cut from a billet by the electric spark method; then it was polished using diamond and finally electrically polished in a NaOH solution. The sample was glued to 2 mm $\times$ 0.5 mm of the working zone of the Hall probe.

A block scheme of the installation is shown in figure 1. The square-wave generator 1, acting as synchronizer, triggers the modulation pulse generator 2, which forms the high-power rectangular pulses. These pulses enter an emitter follower 3. The coaxial line and the sample 4 serve as the loading of the emitter follower. The current contacts of the Hall probe 5 are connected to the oscillator 6, which supplies the probe with the alternating current $J_H = 138$ mA. The frequency f_H of this current was from 20 to 200 Hz. At a given J_H the Hall probe constant k_H is 300 μV mT^{-1}. The signal from the potential contacts of the probe was measured at the frequencies close to the difference frequency between f_H and the repetition frequency F of the current pulses. The measurement was performed using the selective microvoltmeter 7. As a rule, a regime with selectivity as high as 54 dB/octave was used. The time constant τ_f of signal integration was 5 or 0.5 s.

Also, the measurements of the pulse component of magnetic field were made. In that case, the supply for the Hall probe was the direct current $J_H = 100$ mA. The signal from the potential contacts of the probe was amplified by the broad-band amplifier 8 and measured by the gate converter 9. This measurement was fulfilled in a moment when the strobe signal entered from generator 1. That strobe signal was delayed some tens or hundreds of

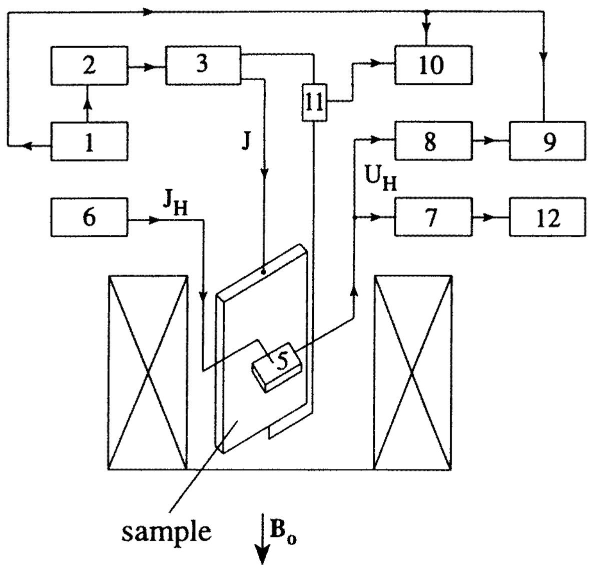

Figure 1. Scheme of the experimental installation.

microseconds from the onset of the current pulse. To separate a useful signal from pulse interference, inversion of the supply current was used.

A voltage from the shunt 11 proportional to the current strength was given to the oscilloscope. The record of the temporal deviations of the signal was realized by recorder 12.

The methods described enable us to determine the current components, which are perpendicular to the z direction, if those components result from the instability. These components induce partial magnetic induction along Oz. Generally, that partial magnetic induction is time dependent. Inasmuch as the instability is caused by the periodic sequence of the current pulses with the repetition frequency F, thus the spectrum component of the magnetic induction of the instability with the lowest frequency becomes of the form $\tilde{B}(t)\sin[2\pi Ft + \varphi(t)]$. Taking into account the steady field of the solenoid, the component B_z can be written as

$$B_z = B_0 + \tilde{B}(t)\sin[2\pi Ft + \varphi(t)]. \tag{1}$$

The supply current of the Hall probe is $i_H = J_H \sin(2\pi f_H t)$. The voltage between the potential contacts of the probe is given by

$$u_H = k_H B_z i_H = k_H B_0 J_H \sin(\omega_H t) + k_H \tilde{B}(t) J_H \sin[\Omega t + \varphi(t)] \sin(\omega_H t) \tag{2}$$

where $\Omega = 2\pi F$ and $\omega_H = 2\pi f_H$. Let us consider the frequency range close to the difference frequency $\Omega - \omega_H$, which is present in the signal spectrum (2). The appropriate voltage is proportional to

$$U|\Omega - \omega_H = k_H \tilde{B}(t) J_H \cos[(\Omega - \omega_H)t + \varphi]. \tag{3}$$

This expression is useful when the instabilities are observed to be more slowly varying than the difference frequency period $2\pi/|\Omega - \omega_H|$.

Efforts were made to prevent the interaction of the current pulse and the external magnetic field. The superconducting solenoid was in persistent mode. The homogeneity of the external field was better than 1%. Because the sample and the massive specimen holder were securely glued, the effect of sample vibration was estimated to be neligible. Much care has been taken to avoid asymmetric components of the current with no applied magnetic field. The tungsten plate was placed between two contacts whose width just exceeds the sample's width. The intimate mating of the contacts to the sample was provided by indium gaskets. The Hall probe signal was zero within the experimental accuracy of about 0.1 μV when the magnetic field was absent.

To record the elastic displacement a piezoelectric ceramic transducer was glued alongside the Hall probe. The resonance frequency of the transducer was 30 kHz. The signal from the transducer was passed through the amplifier and could be observed with the oscilloscope.

3. Results

When strong current pulses pass through the tungsten plate longitudinally to the external magnetic field, the z component of the pulse magnetic field appears (figure 2). The oscillograms of the current pulse amplitude J and strobe signal st are shown in the inset. In figure 2(a) a section is presented of the time dependence of the Hall probe voltage; the onset of the strobe signal is the reference point. The data in figure 2 were obtained when $B_0 = 7$ T and $J_M = 80$ A. The existance of the z component of the magnetic field, which exceeded 3 Oe, testifies to the appearance of a perpendicular current. This instability current are circulating inside the sample and has an order of magnitude of hundreds of milliamperes. As was established, the lifetime of the transverse currents after one pulse can be as high as 7 ms. The magnitude of the Hall probe voltage changes from one current pulse to another. The envelope of those deviations have a non-periodic oscillational character (figure 2(b)). By this it is meant that the instability transient currents are retained as fluctuations up to the onset of the next pulse.

To determine the exposure of the instability threshold in the current amplitude the Hall probe voltage was measured at the difference frequency. The experiments conducted showed that, when $\boldsymbol{J} \parallel \boldsymbol{B}_0$, if the current pulse is sufficiently strong, then an alternating magnetic field arises with the difference frequency $\Omega - \omega_H$. The dependence of the Hall probe voltage, which is proportional to that field, on the current amplitude J_M (figure 3(a)), represents a function having the threshold current amplitude J_t. This function rises sharply when the threshold J_t is exceeded. The Hall voltage $U|\Omega - \omega_H$ is absent at $B_0 = 0$; it slowly increases, when B_0 increases up to some value. Then a sharp increase is realized (inset in figure 3(a)). Either simultaneously with this event or at a higher B_0, oscillational deviations arise in the Hall probe voltage with time. The range of deviations is shown by the broken curve in the inset of figure 3(a). The appearance of the voltage $U|\Omega - \omega_H$ is caused by the z component of the magnetic field with frequency $\Omega - \omega_H$. The dependence of the threshold value on B_0 is shown in figure 3(b). The measurements in figure 3 are for the following conditions: $\tau_J = 60$ μs, $f_H = 200$ Hz and $f_H - F = 12.3$ Hz, except for the inset, where $f_H = 85$ Hz, $F = 80$ Hz and $\tau_J = 94$ μs.

The voltage amplitude varies from one current pulse to the next. These changes are oscillational over a time interval of seconds and contain a wide frequency spectrum beginning from 0.01 Hz and finishing at tens hertz, at least. The long-time deviations, which are recorded at the integration constant $\tau_f = 5$ s, are presented in figure 4 for various values of magnetic induction. The picture of the oscillations in the amplitude ΔU that is recorded on a comparatively small time scale is shown in figure 3(a); here $B_0 = 6$ T and

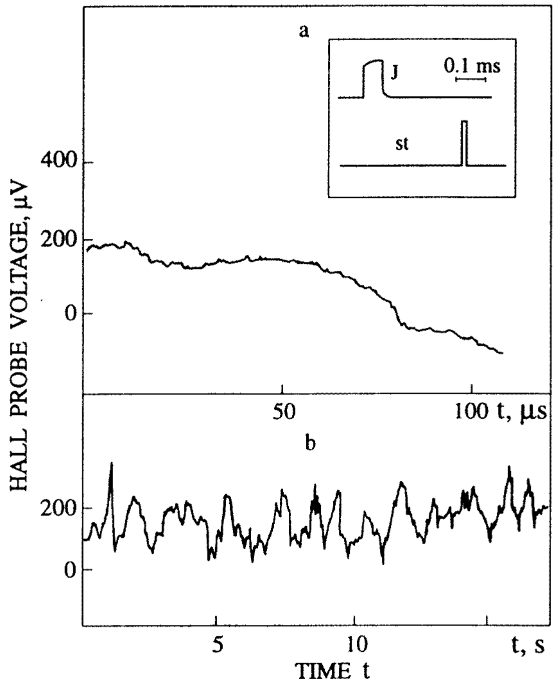

Figure 2. Time dependence of (a) the Hall probe voltage and (b) the amplitude of gated probe voltage; in the inset, oscillograms of the current pulse and strobe signal are shown.

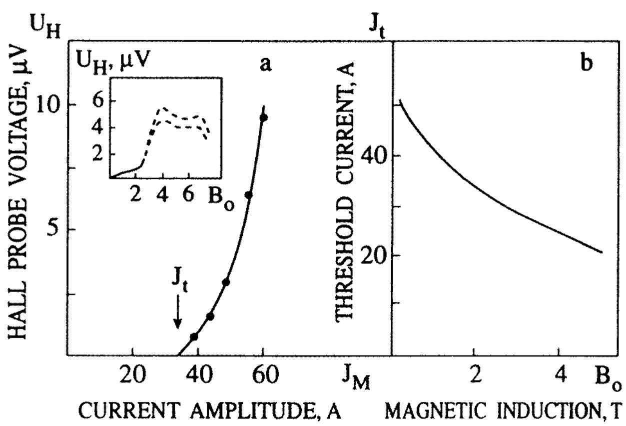

Figure 3. (a) Hall probe voltage versus current asmplitude J_M and (b) threshold current amplitude versus magnetic induction; in the inset, the magnetic field dependence of the Hall probe voltage is shown.

$\tau_f = 0.5$ s. For the dependences obtained when the current strength is near the threshold value, the intervals have obvious weak amplitude deviations (which are laminar periods) and the intervals of sharp oscillations. At high values of the pulse currents the laminar periods become shortened, giving way to the developed turbulence. This picture recalls

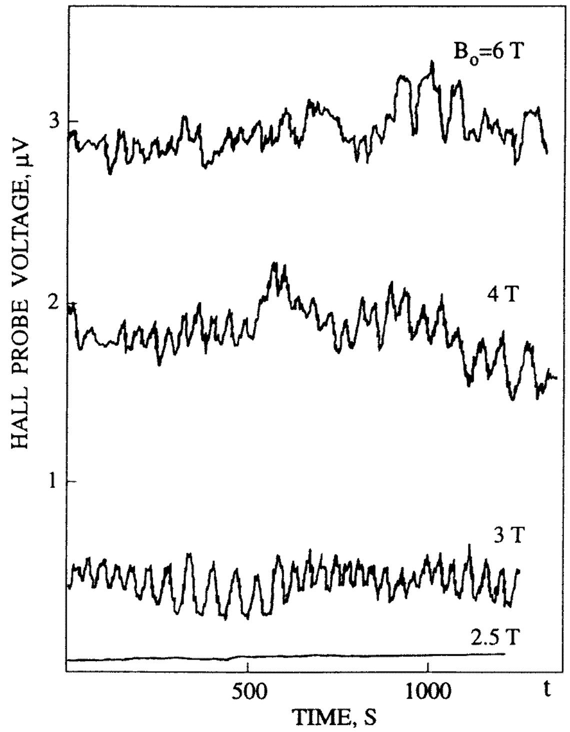

Figure 4. The long-time deviations of the probe voltage ($J_M = 50$ A; $f_H - F = 3.5$ Hz).

the change in the system to dynamical chaos following the intermittency scenario [12]. The linear dependence of the mean time interval of the laminar gaps on the parameter $[(J_M - J_t)/J_t]^{1/2}$ shows the validity of this assumption (figure 5(b)).

Simultaneously with the measurements of the instability, elastic oscillations of the tungsten plate were obtained. The elastic displacement component was measured normally to the plate plane. The measurements were carried out at the resonant frequency of the transducer, 30 kHz; the results are shown in figure 6. Hence, it should be emphasized that the elastic oscillations of the plate arise in conditions of instability.

4. Discussion

In this section some explanations for the of instability appearance of the pulse current in a longitudinal magnetic field should be given, taking into account the experimental results. The most significant of these are

(1) the appearance of the transverse component of the instability currents, which are circulating inside the sample,

(2) the oscillational characteristic as well as the low frequency of these currents,

(3) the existence of a threshold for the instability and

(4) the appearance of elastic oscillations.

In the discussion we shall follow the review paper [13], where corrections are introduced relevant to our experimental conditions.

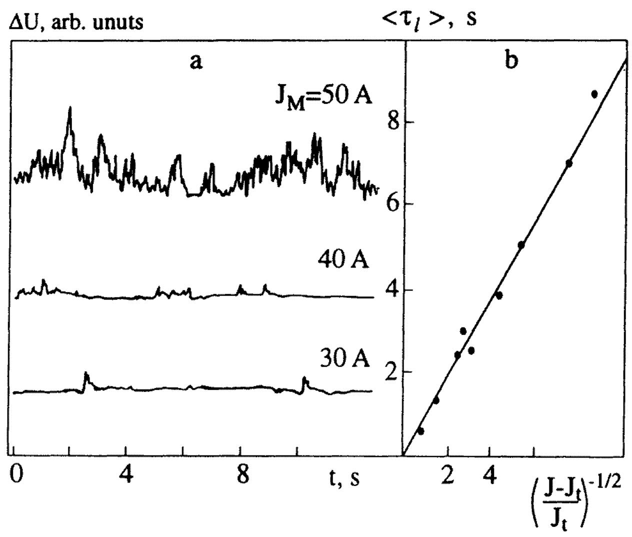

Figure 5. (a) Deviations of the probe voltage; (b) mean time interval of the laminar periods of the probe deviations.

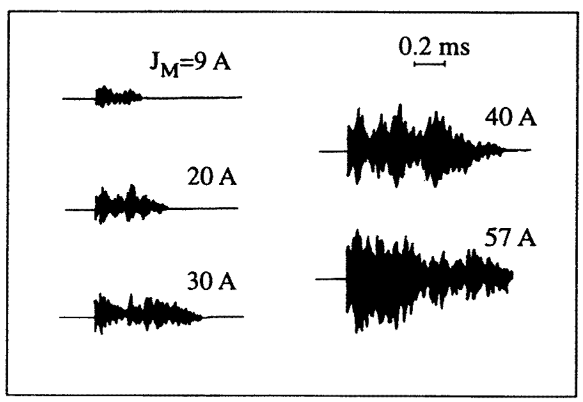

Figure 6. The oscillograms of the signals from the elastic transducer at $B_0 = 6$ T.

Assume that the external magnetic field $\boldsymbol{H}_0$ is parallel to the current $\boldsymbol{J}$. The current pulses create at the plate boundary the magnetic field H_s, which is parallel to the y axis. The frequencies of this field are in accordance with the frequencies ω_s of the spectrum of the current pulses. Let us assume that the anomalous skin-effect condition is fulfilled at the frequencies ω_s. Also, we suppose the inequality $\omega_s \ll \nu$ to be true, where ν is the scattering frequency of the electrons. When $R_s = p_F/eH_s \ll l$ (R_s is the cyclotron radius in the field H_s of the pulse current, l is the electron mean free path and p_F is the Fermi momentum), the connection between the electric field and current may be taken as local. If one use Maxwell equations for the curls of the fields, the following parabolic-type equation will be obtained for the electromagnetic field in a metal:

$$\sigma_0 \frac{R_s^2}{l^2} \frac{\partial \kappa}{\partial t} = \frac{\partial}{\partial x}\left(\kappa^2 \frac{\partial \kappa}{\partial x}\right) + \frac{\partial}{\partial z}\left(\kappa_0^2 \frac{\partial \kappa}{\partial x}\right) \tag{4}$$

where σ_0 is the direct-current conductivity of the metal, $\kappa = H/2H_s$ is the normalized amplitude of the alternating magnetic field H in metal (where the induced component is included) and $\kappa_0 = H_0/2H_s$. The x axis of the coordinate system is directed along the normal to the plate plane; the origin is placed at the centre of the plate. On both sides of this plate the effective boundary conditions are written for the electric field $\boldsymbol{E}$:

$$E_z\left(\frac{\pm d}{2, z, t}\right) = \mp 2H_s \frac{\omega_s \delta_s}{c} \Phi(\kappa(t), \boldsymbol{H}_0). \tag{5}$$

In equation (5), δ_s is the skin depth at the frequency ω_s. The function $\Phi(\kappa(t), \boldsymbol{H}_0)$ depends on the mechanism of formation of the induced field $\boldsymbol{h}$. For the situation discussed with $\boldsymbol{J} \parallel \boldsymbol{H}_0$, $H_0 \gg H_s$; the form of this function has not been obtained theoretically yet. In all the instances previously considered [13, 14], the function $\Phi(\kappa)$ becomes non-monotonic when the amplitude of the incident magnetic field exceeds a certain critical value, $H_s > H_{cr}$. As this takes place, an interval appears for the dependence $\Phi(\kappa)$, where $\Phi' = \partial\Phi/\partial\kappa > 0$. We shall presuppose this form of the $\Phi(\kappa)$ dependence also in our case. Under the condition $\Phi' > 0$ the electrodynamical system becomes unsteady; spatial $\tilde{\delta}$ and temporal $2\pi/\tilde{\omega}$ scales of the fields deviations arise, while the energy flow is directed inside the metal [14]. We restrict our attention to the instabilities which are uniform along the y axis. Let us introduce the parameters

$$\tau_\kappa = d/\omega_s \delta_s \qquad \tilde{\delta} = \delta_s (l^2 d/R_s^3)^{1/2}. \tag{6}$$

We then carry out averaging along the x axis and rewrite equation (4) as

$$\tau_\kappa \frac{\partial \kappa}{\partial t} = \tilde{\delta}^2 \kappa_0^2 \frac{\partial^2 \kappa}{\partial z^2} + \Phi(\kappa). \tag{7}$$

As was shown in [14], equation (7) has a steady solution of switching wave type travelling in the plate. In our case when a high-intensity electromagnetic field is created by the electric current, equations (4) and (5) should be supplemented by the equation for current changes. According to [10], a trapped group of the electrons exists in the metal plate through which the current flows under the $\boldsymbol{H}_0 \parallel \boldsymbol{J}$ condition. This electron group transfers the current J_{tr}. The currents in the transmitting line with distributed parameters obey the telegraph equations, in which the inductance L_0 and capacitance C_0 per unit length occur. If the frequency is very low, then $\omega_0 = (L_0 C_0)^{-1}$, and the telegraph equation for the current is reduced to the following form:

$$\tau_{em} \frac{\partial J_{tr}}{\partial t} = -J_{tr} + J + \frac{V}{L} \delta_s \sigma_0 D \tag{8}$$

where J is the current in the outer circuit, V is the voltage drop at the sample, L and D are the length and width, respectively of the metal plate, and $\tau_{em} = L_0 \sigma_0 D d$. Equation (8) is the same as the equation obtained in [15]. Using (8) jointly with (5) and (7) changes the behaviour of the system radically, providing the recovery mechanism in the initial state after the switching wave has passed. As a result the system (5), (7), (8) has an oscillational-type solution.

The transmission of energy inside a metal under the condition $\Phi' > 0$ as well as the existence of the trapped electron group with the negative differential resistance permit instability realization in the metal plate. The conditions of instability in the objects described by an equation system similar to (7), (8) have been considered in [15]. The criterion of long-wavelength instability from [15] in our case is

$$\frac{\partial\Phi(\kappa)}{\partial\kappa} > \frac{\tau_\kappa}{\tau_{em}}. \tag{9}$$

In the conditions of the experiments being discussed, $\tau_\kappa = 10^{-8}$ s, $\tau_{em} = 10^{-6}$–10^{-7} s. By virtue of the fact that $\tau_\kappa < \tau_{em}$ the inequality (9) is near to

$$\Phi'(\kappa) > 0. \tag{10}$$

A necessary condition for the validity of this inequality is that the magnetic field amplitude caused by the current exceeds a certain critical value: $H_s > H_{cr}$. When the field equals the critical field, the arc length of the electron trajectory in the magnetic field H_s becomes shorter than the mean electron free path. This corresponds to the condition

$$b_{cr} = \frac{2H_s el^2}{8cp_F\delta_s(H_s)} \geqslant 1 \tag{11}$$

where the dependence of the skin depth δ_s on the field H_s must be taken into account. The evaluation gives $H_s \simeq 10$–20 Oe at $\delta_s \simeq 10^{-3}$ cm and $l \simeq 0.1$ cm. Fields of this order are the origin of the threshold currents J_t observed experimentally. The considerations above assume the validity of the inequality $H_0 \gg H_s$ and the existence of the trapped electron group. In these limits an analysis of the threshold current dependence on the external magnetic field intensity is quite impossible. That analysis has been made possible only after the function $\Phi(\kappa(t), \boldsymbol{H}_0)$ has been obtained in an explicit form.

Instability in the distribution of the direct current in the longitudinal magnetic field was predicted in [10]. The voltage–current characteristic of the metal plate is in the form of a curve that has a maximum and a minimum. The decreasing part of this curve is connected to the negative differential resistance due to the trapped electrons. The instability appears if the current strength exceeds the value corresponding to the maximum of the voltage–current characteristic. This type of instability, in principle, exists also for the pulse current. For the estimations, however, it must be noted that the pulse current is concentrated inside the skin depth δ_s. Therefore, for a qualitative evaluation we need to insert δ_s instead of the plate thickness d in the expression for the voltage–current characteristic. For $\delta_s = 3 \times 10^{-4}$ cm, $l = 0.1$ cm and $H_0 = 32$ kOe, the maximum of the characteristic accounted for the value $H_s = 550$ Oe. This exceeds considerably the quantities realized in our experiment. Beyond that point the instability [10] is expressed in the appearance of the x component of the magnetic field, but in fact the z component is observed. From the result obtained, it may be inferred that the latent negative differential resistance of the trapped electrons leads to instability of the pulse current well before the descreasing part of the voltage–current characteristic is achieved.

The appearance of the alternating magnetic field, and therefore the currents that are perpendicular to the z axis, under the instability conditions can be explained by a mechanism similar to the current–convective instability in a gas plasma or the helical instability in a semiconductor plasma. The alignment of the current and external magnetic field in our experiment is the same as for these instabilities. Either a charge density gradient or a magnetic field gradient remains in the plasma as a necessary condition for this type of instability. The inhomogeneity of the magnetic field originates in our case from the field of the pulse current localized on the spatial scale δ_s in the metal. From the Maxwell equation for the divergence of magnetic induction, it may be deduced that the variation in the y component of the magnetic field of the instability causes the z component to appear.

An explicit form of the function $\Phi(\kappa, \boldsymbol{H}_0)$ is required for numerical estimations of the z component.

It is known that the type of instability discussed is possible in a compensated metal in two instances [16]. The electrical neutrality condition will be obeyed either when the mobilities of electrons and holes differ dramatically, or when elastic oscillations are excited. As may be inferred from figure 6, the second possibility is realized in the tungsten plate.

5. Conclusion

It should be pointed out that the detection of a strong pulse current instability in a metal plate in a longitudinal magnetic field is a particularly interesting experimental result. The time-dependent contribution to the z component of the magnetic field arises as a result of the instability. This instability is accompanied by elastic oscillations. The system examined undergoes a change to the dynamic chaos regime via intermittency.

A set of equations is proposed, which prescribe the oscillational changes in the current and magnetic field. This system is based on the magnetodynamical origin of the interaction. The criterion of long-wavelength instability is established. The latent negative differential resistance of the trapped electrons was demonstrated to have the pulse current instability at a lower current than in the case of the direct current.

Acknowledgments

The authors are grateful to Dr R Nasyrov and Mr V Manakov for the provision of the high-purity tungsten single crystal.

References

[1] Azbel M Ya 1969 *Pis. Zh. Eksp. Teor. Fiz.* **10** 550
[2] Zhilyaev I N 1992 *Pis. Zh. Eksp. Teor. Fiz.* **55** 727
[3] Kopylov V N 1981 *Fiz. Tverd. Tela* **23** 1948
[4] Esaki L 1962 *Phys. Rev. Lett.* **8** 4
[5] Pestchansky V G and Stepanenko D L 1991 *Pis. Zh. Eksp. Teor. Fiz.* **54** 329
[6] Marchenkov V V, Cherepanov A N and Startsev V E 1992 *Fiz. Metall. Metalloved* No 2 35
[7] Kaner E A, Makarov N M, Snapiro I B and Yampolsky V A 1984 *Zh. Eksp. Teor. Fiz.* **87** 2166
[8] Zakharchenko S I, Kravchenko S V and Fisher L M 1986 *Zh. Eksp. Teor. Fiz* **91** 660
[9] Makarov N M, Tkachev G B and Yampol'skii V A 1994 *Proc. 30th Russ. Conf. on Low Temperature Physics (Dubna, 1994)* part 2 (Dubna: Joint Institute for Nuclear Research) p 277
[10] Kaner E A, Makarov N M, Snapiro I B and Yampolsky V A 1985 *Zh. Eksp. Teor. Fiz.* **88** 1310
[11] Voloshin I F, Kravchenko S V, Podlevskikh N A and Fisher L M 1985 *Zh. Eksp. Teor. Fiz.* **89** 233
[12] Manneville P and Pomeau Y 1980 *Physica* D **1** 219
[13] Makarov N M and Yampol'skii V A 1991 *Fiz. Niz. Temp.* **17** 547
[14] Kaner E A, Makarov N M, Yurkevich I V and Yampolsky V A 1987 *Zh. Eksp. Teor. Fiz.* **93** 274
[15] Kerner B S and Osipov V V 1991 *Autosolitons* (Moscow: Nauka)
[16] Kaner E A and Yakovenko V M 1975 *Usp. Fiz. Nauk.* **115** 41